Research Square

Preprints are preliminary reports that have not undergone peer review.
They should not be considered conclusive, used to inform clinical practice,
or referenced by the media as validated information.

Chitosan-Coated 5-FU Liposomal Gel for Enhanced Skin Melanoma Treatment: Multi- Model Evaluation

Muhammad Khurshid Alam Shah
Gomal University
Waseem Mehmood
Gomal University
Haroon Khan
Gomal University
Muhammad Fauzi Abd Jalil
University of Malaya
Riyanto Teguh Widoodo
University of Malaya
Asif Nawaz
University of Malaya
Mulham Alfatama
Sultan Zainal Abidin University
Hazem Choukaife
hazemchoukaife@uitm.edu.my

Universiti Teknologi MARA

Research Article

Keywords: Liposomes, Chitosan, 5-fluorouracil, Melanoma, Dermal Delivery

Posted Date: November 20th, 2026

DOI: https://doi.org/10.21203/rs.3.rs-11452965/v1

License: This work is licensed under a Creative Commons Attribution 4.0 International License.
Read Full License

Additional Declarations: No competing interests reported.

Chitosan-Coated 5-FU Liposomal Gel for Enhanced Skin Melanoma Treatment: Multi-Model Evaluation

Muhammad Khurshid Alam Shah [1], Waseem Mehmood[1], Haroon Khan[1], Muhammad Fauzi Abd Jalil[2], Riyanto Teguh Widoodo[2], Asif Nawaz[1,2]*, Mulham Alfatama[3]*, Hazem Choukaife[4]*

[1] Gomal Center of Pharmaceutical Sciences, Faculty of Pharmacy Gomal University Dera Ismail Khan, 29050, Pakistan.
[2] Department of Pharmaceutical Technology, Faculty of Pharmacy, Universiti Malaya, Kuala Lumpur, Malaysia.
[3] Faculty of Pharmacy, Universiti Sultan Zainal Abidin, Besut Campus, Besut 22200, Terengganu, Malaysia
[4] Faculty of Pharmacy, Universiti Teknologi MARA (UiTM) Cawangan Selangor, Kampus Puncak Alam, 42300 Bandar Puncak Alam, Selangor Darul Ehsan, Malaysia.

***Corresponding Author**: Hazem Choukaife (hazemchoukaife@gmail.com), Mulham Alfatama (mulham4122@yahoo.com), Asif Nawaz (asifnawaz@um.edu.my)

Abstract

Chitosan-functionalized liposomes have emerged as attractive lipid–polymer carriers for enhancing the cutaneous administration of anticancer drugs. In this work, 5-fluorouracil (5-FU) was incorporated into conventional and chitosan-coated liposomal systems intended for topical melanoma therapy. The developed formulations were evaluated for vesicle size, polydispersity index (PDI), surface charge, entrapment efficiency (EE%), drug loading (DL%), morphology, and storage stability. Their delivery performance was subsequently examined through *in vitro* release studies, *ex vivo* skin permeation and retention experiments, ATR-FTIR characterization, and cytotoxicity testing against SK-MEL-28 melanoma cells. The developed vesicles exhibited a spherical morphology with relatively smooth surfaces, while chitosan coating increased vesicle size and altered the surface charge toward a more positive potential. Surface modification with chitosan also improved physical stability, drug entrapment, skin permeation, and cutaneous retention compared with uncoated liposomes. ATR-FTIR findings indicated physicochemical compatibility among 5-FU and the formulation components without evidence of major chemical alteration. Among the tested systems, the chitosan-coated liposomal gel demonstrated the strongest cytotoxic activity against SK-MEL-28 cells, together with superior skin permeation and drug retention. Overall, the findings suggest that combining liposomal encapsulation with chitosan coating and gel incorporation can enhance the topical delivery and anticancer performance of 5-

FU, supporting the potential of this lipid–polymer hybrid system as a promising platform for localized melanoma therapy.

Keywords: Liposomes; Chitosan; 5-fluorouracil; Melanoma; Dermal Delivery

1.0 Introduction

Skin cancer melanoma is the most common disease in United State and Europe, and is accountable for the majority of the skin tumor related fatalities [1]. Skin melanoma therapy includes surgical intervention, chemotherapy, and radiotherapy. The presence of residual tumor cells may instigate tumor recurrence leading to failure of surgical therapy [2]. Therefore, chemotherapy is commonly administered as an adjuvant treatment following surgical removal of tumors. However, conventional chemotherapeutic approaches are often associated with severe systemic toxicity, the emergence of multidrug resistance, and reduced therapeutic efficacy [3]. Hence, the development of safe and effective chemotherapeutic strategies with minimal side effects and reduced invasiveness is essential. Localized drug delivery to the skin represents a promising approach to mitigate the systemic toxicity associated with antitumor agents and to enhance their therapeutic efficacy.

The skin, as the body's largest organ, provides an accessible site for localized therapeutic intervention in cutaneous malignancies. Transdermal delivery offers a non-invasive alternative to oral and parenteral administration by allowing drugs to cross the skin barrier without the need for needles or tissue injury. This approach can circumvent several limitations associated with gastrointestinal delivery, including variations in gastric pH and emptying, enzymatic degradation, and first-pass hepatic metabolism. In addition, topical administration offers practical advantages because treatment can be readily terminated by removing the formulation from the application site [4]. A major challenge in topical and transdermal delivery is the limited permeability of the skin, primarily because the stratum corneum acts as a highly effective barrier to the passage of most therapeutic molecules. To overcome this restriction, a wide range of physical and chemical permeation-enhancement approaches have been explored to modify barrier properties and improve drug transport into or across the skin [5]. Recently, novel topical formulations have been explored to modulate the skin's barrier properties for enhanced drug penetration [6]. Advanced delivery systems such as magnetic core–shell structures, nanoemulsions, nanoparticles, liposomes, and nanofibers, have been investigated for transdermal administration in the treatment of melanoma [7].

Liposomes are spherical vesicular nanoparticles composed of one or more lipid bilayers primarily made up of phospholipids and cholesterol [8]. Their unique lipid composition and aqueous core impart an amphiphilic nature, allowing the encapsulation of both hydrophilic and lipophilic drugs. Moreover, liposomes exhibit excellent biocompatibility, biodegradability, non-immunogenicity, and low toxicity, making them highly suitable for pharmaceutical and biomedical applications [9]. In recent years, liposomes have been increasingly employed in antitumor applications, progressing from laboratory-scale studies to the development of commercially available formulations [10]. However, their clinical utility remains limited by inherent drawbacks such as aggregation and fusion, which can lead to premature drug leakage during storage [11]. Furthermore, liposomes are susceptible to degradation under varying pH conditions, enzymatic activity, and immune system interactions [12]. To address these limitations, structural modification of liposomes through polymer incorporation has been investigated. The integration of polymers enhances the physicochemical stability, mechanical strength, and overall performance of liposomal formulations [13].

Natural biopolymers are increasingly incorporated into pharmaceutical delivery systems because they combine functional versatility with favorable biological properties. Chitosan is one of the most widely investigated materials in this context and is commonly employed as a carrier, coating agent, and formulation excipient. Structurally, it is a positively charged amino-polysaccharide obtained by partial deacetylation of chitin, which is naturally abundant in crustacean exoskeletons and fungal cell walls. Its pharmaceutical relevance is supported by its biodegradability, biocompatibility, and low toxicity. Beyond these material characteristics, chitosan has also been associated with antimicrobial, antioxidant, anti-inflammatory, and antitumor activities, making it particularly attractive for the design of multifunctional drug delivery systems [14]. Chitosan interacts electrostatically with negatively charged liposomes through the attraction between the anionic phospholipid head groups and the cationic primary amino groups of chitosan [15]. In addition to electrostatic interactions, hydrogen bonding between chitosan and phospholipid head groups further contributes to the formation of a stable chitosan coating. Chitosan-coated liposomes exhibit enhanced physicochemical stability, improved bioavailability of the encapsulated drug, and greater membrane flexibility compared to uncoated liposomes. These attributes make them a promising delivery system for drugs with poor permeability or those associated with adverse side effects. Therefore, the present study investigates the effectiveness of chitosan-coated liposomal

formulations in facilitating transdermal delivery and enhancing drug penetration into melanoma cells. The potential of combining natural polymers such as chitosan with liposomal systems for skin-targeted drug delivery and melanoma therapy is also evaluated .

2.1 Materials

Cholesterol, 5-fluorouracil (5-FU), and low-molecular-weight chitosan with a degree of deacetylation of 92% were obtained from Sigma-Aldrich Chemical Co. Ltd. (St. Louis, MO, USA). Glacial acetic acid, polysorbate 80, and sodium tripolyphosphate (TPP) were purchased from BDH Organic (Poole, Dorset, UK), while soybean lecithin containing >94% phosphatidylcholine was supplied by Lipoid GmbH (Ludwigshafen, Germany). Carbomer, triethanolamine, propylparaben, methylparaben, and chloroform were also sourced from Lipoid GmbH. Anhydrous disodium hydrogen phosphate (Na_2HPO_4) and sodium dihydrogen phosphate monohydrate were used for preparation of the buffer solutions. Unless otherwise stated, all reagents were of analytical grade and were used as received without additional purification.

2.2 Preparation of Liposomes

5-FU-loaded liposomes were fabricated using a lipid-film hydration procedure with subsequent sonication and membrane extrusion. Soybean lecithin and cholesterol were dissolved in chloroform, and the solvent was evaporated under reduced pressure at 40–45 °C to generate a thin lipid layer on the inner surface of a round-bottom flask. The resulting film was kept under vacuum overnight to remove residual organic solvent. Hydration was then carried out at 40 °C using phosphate-buffered saline (PBS, pH 7.4) containing 5-FU under continuous mixing, producing multilamellar vesicles. The vesicular dispersion was further processed by probe sonication for 5–10 min under ice-bath conditions and extruded through 120 nm polycarbonate membranes to obtain smaller vesicles with improved size uniformity [16].

Chitosan-coated liposomes were prepared through electrostatic deposition of the cationic polymer onto the liposomal surface. Chitosan was dissolved at 0.6% (w/v) in 0.5% (v/v) glacial acetic acid and stirred continuously for 2 h until a clear and homogeneous solution was obtained. The chitosan solution was then added dropwise to an equal volume of liposomal dispersion containing 5% dextrose under continuous stirring for 60 min. This gradual addition promoted electrostatic interaction between the positively charged chitosan chains and the oppositely charged liposomal

surface, resulting in the formation of a uniform polymeric coating around the vesicles. The coated dispersion was subsequently stored overnight at 4 °C to enhance stabilization of the chitosan layer. Finally, the chitosan-coated liposomes were collected by centrifugation at 15,000 × g for 30 min at 4 °C and stored under refrigerated conditions until further characterization and use [17].

2.2.1 Liposomal gel Preparation

For preparation of the liposomal gel, Carbopol 940 was dispersed in distilled water at a concentration of 1% (w/v) and left to hydrate for 24 h. Following complete swelling of the polymer, triethanolamine was gradually incorporated under continuous stirring until the formulation reached pH 5.5, thereby producing a homogeneous gel base. The chitosan-coated liposomal dispersion was then carefully blended with the hydrated Carbopol matrix using gentle agitation to minimize possible damage to the vesicular structure. Subsequent homogenization was performed to promote even distribution of the liposomes throughout the gel network. The resulting chitosan-coated 5-FU liposomal gel was transferred into airtight containers and maintained at 4 °C prior to further evaluation. The qualitative and quantitative compositions of the blank and 5-FU-loaded liposomal formulations are presented in Table 1.

2.3 Physicochemical characterization of liposomes and liposomal gel

2.3.1 Particle size and Zeta Potential Analysis

The mean particle size and zeta potential of the BL, F1, and F2 liposomal formulations were determined by dynamic light scattering (DLS) using a Malvern Zetasizer (Malvern Instruments, UK). Basically, these formulations exist as colloidal dispersions. Formulations F3 and F4 are semisolid gel systems in which liposomes are encapsulated in a three-dimensional polymeric network. The restricted mobility of vesicles and interference from the gel matrix make standard DLS techniques ineffective for measuring these parameters. Consequently, only the precursor liposomal formulations were studied for vesicle characterization. Therefore, the parameters for F3 and F4 were not evaluated, and vesicle characterization was limited to precursor liposomal formulations. Before measurement, each sample was appropriately diluted with deionized water and gently vortexed to obtain a uniform dispersion. Zeta potential was determined by transferring the diluted samples into an electrophoretic cell and measuring under standard instrument settings. Each analysis was conducted in triplicate, with the data reported as mean ± standard deviation

(SD). This study has limitations in that vesicle size and surface charge were not directly evaluated after incorporation into gel formulations (F3 and F4). Due to methodological constraints associated with semisolid systems, such measurements may not accurately reflect liposome structures within gel matrixes.

2.3.2 Drug Content and Entrapment Efficiency (%)

Drug entrapment efficiency and loading capacity were determined by dispersing 1 g of the liposomal formulation in 99 mL of phosphate buffer (pH 7.4), followed by continuous magnetic stirring for 2 h. The dispersion was subsequently centrifuged at 5000 rpm for 2 h to separate the unencapsulated drug from the liposome-associated fraction. The supernatant was collected and analyzed by UV–visible spectrophotometry at 260 nm to quantify the free 5-FU. The liposomal pellet was then dissolved in ethanol to disrupt the vesicles and release the entrapped drug, which was quantified using the same analytical procedure. Entrapment efficiency and drug loading were calculated using the corresponding equations:

$$Drug\ Loading\ (\%) = \frac{Amount\ of\ drug\ entrapped}{Total\ weight\ of\ liposomes} \times 100$$

$$\text{Entrapment efficiency } (\%) = \frac{Amount\ of\ drug\ entrapped}{Total\ drug\ added} \times 100$$

2.3.3 Scanning electron microscopy

The morphology of the liposomal vesicles was characterized by scanning electron microscopy (SEM) using a JEOL JMS-840 instrument. Before analysis, the samples were freeze-dried, placed on aluminum specimen stubs, and sputter-coated with a thin gold layer to improve electrical conductivity. The prepared specimens were subsequently examined by SEM to evaluate vesicle morphology, including particle shape, surface architecture, and apparent size [11].

2.3.4 ATR-FTIR analysis

Attenuated Total Reflectance–Fourier Transform Infrared (ATR-FTIR) spectroscopy was conducted to confirm the identity of individual components and evaluate possible intermolecular interactions within the liposomal formulations. The infrared spectra of cholesterol, soybean

lecithin, chitosan, 5-fluorouracil (5-FU), and the prepared liposomal systems were recorded using a Fourier Transform Infrared Spectrophotometer (IRPrestige-21, Shimadzu, Tokyo, Japan) equipped with an ATR accessory. Each sample was scanned within the wavenumber range of 400–4000 cm^{-1} at a spectral resolution of 4 cm^{-1}, with 28 co-added scans collected under ambient conditions. The characteristic absorption peaks were identified and analyzed using IR Solution software (version 1.40).

2.3.5 Physical stability studies

The storage stability of the developed liposomal formulations was assessed over 30 days under refrigerated (4 ± 1 °C) and ambient (25 ± 2 °C) conditions at 60 ± 5% relative humidity, in accordance with ICH recommendations. Samples were maintained in a controlled stability chamber (NuAire, Plymouth, MN, USA) and analyzed at predetermined intervals. Stability was evaluated by monitoring changes in vesicle size, polydispersity index (PDI), and entrapment efficiency throughout the storage period. All measurements were performed in triplicate to assess the physicochemical and colloidal stability of the formulations over time [18, 19].

2.3.6 Skin Irritation Test

The dermal tolerability of the developed liposomal formulations was examined in male Sprague–Dawley rats weighing 200–250 g. Ethical clearance for the study was obtained from the Gomal Centre of Pharmaceutical Sciences, Faculty of Pharmacy, Gomal University, Dera Ismail Khan, Khyber Pakhtunkhwa, Pakistan (Approval No. 518/ERB/GU). All animal procedures were conducted in compliance with institutional ethical standards and ARRIVE recommendations.

Prior to treatment, the animals were acclimatized under controlled conditions of 25 ± 2 °C, 50–60% relative humidity, and a 12 h light/dark cycle, with free access to food and water. Thirty-six rats were randomly assigned to six groups (n = 6). Group 1 served as the untreated negative control, whereas Groups 2–5 received a single 1 mL topical application of the respective formulation on the left auricle; the untreated right auricle was used as an internal control. Formalin was applied to Group 6 as a positive control for irritation.

After application, the treated areas were monitored at predetermined times over 24 h for visible signs of erythema and edema. The severity of the local reaction was graded on a five-point scale

from 0 to 4, corresponding to no reaction, slight, well-defined, moderate, and severe irritation, respectively, with the highest score also encompassing possible scarring [20].

2.4. *In-vitro* release studies

The *in vitro* release of 5-fluorouracil (5-FU) from the developed formulations was investigated using Franz diffusion cells according to a modified previously reported method [21]. A Tuffryn membrane with an approximate pore size of 0.22 μm was mounted between the donor and receptor compartments. Approximately 1 g of each formulation was placed in the donor chamber, while phosphate buffer (pH 5.5) served as the receptor medium. The system was maintained at 32 °C under continuous stirring at 100 rpm. At predetermined intervals 2 mL samples were withdrawn from the receptor compartment and immediately replaced with an equal volume of fresh buffer to maintain sink conditions. The amount of 5-FU released was quantified by UV–visible spectrophotometry at 260 nm using the corresponding calibration-curve equation. Cumulative drug release was expressed as a percentage of the initial drug content. The resulting release profiles were further fitted to various kinetic models to identify the best-fitting model and elucidate the predominant mechanism governing drug release.

2.5. *Ex-vivo* permeation studies

The *ex vivo* permeation of 5-fluorouracil (5-FU) through rat skin was evaluated using Franz diffusion cells under a protocol approved by the Gomal University Ethics Review Board [18]. Dorsal skin was excised from male Sprague–Dawley rats after careful removal of the hair using an electric clipper followed by gentle shaving to preserve epidermal integrity. After euthanasia, the skin was rinsed with 0.9% saline, and adhering subcutaneous tissue was carefully removed. The prepared skin samples were stored at 4 °C until use.

For the permeation experiment, the skin was mounted between the donor and receptor compartments with the stratum corneum facing the donor chamber. The receptor compartment was filled with phosphate buffer (pH 7.4) and maintained at 37 ± 0.5 °C under continuous stirring at 100 rpm. Approximately 1 g of each formulation was placed in the donor compartment. At predetermined intervals of 0, 0.5, 1, 2, 4, 8, 12, 16, 20, and 24 h, 2 mL samples were withdrawn from the receptor medium and immediately replaced with an equal volume of fresh buffer. The amount of permeated 5-FU was quantified by UV–visible spectrophotometry at 260 nm. All

experiments were performed in triplicate, and the data were expressed as mean ± standard deviation (SD) [21].

2.6. Skin ATR- FTIR Analysis

ATR-FTIR spectroscopy was employed to examine molecular alterations in the skin following exposure to the liposomal formulations [19]. At the end of the *ex vivo* permeation study, the skin samples were retrieved from the Franz diffusion cells and rinsed thoroughly with phosphate buffer (pH 7.4) to remove any formulation remaining on the surface. Each specimen was then placed onto a zinc selenide (ZnSe) crystal for direct spectral measurement. The spectra were collected between 400 and 4000 cm^{-1} using a resolution of 16 cm^{-1}, with an acquisition time of approximately 1.5 min per sample [22].

2.7. Skin drug retention studies

After ATR-FTIR analysis, the skin samples were rinsed repeatedly with 0.9% saline to eliminate residual 5-FU from the tissue surface. The cleaned specimens were cut into small pieces and transferred into phosphate buffer (pH 7.4). Drug extraction was promoted by continuous magnetic stirring, followed by tissue homogenization for 2 min. The homogenized samples were then centrifuged at 5000 rpm for 5 min, and the resulting supernatant was collected. The quantity of 5-fluorouracil retained within the skin tissue was subsequently measured by UV–visible spectrophotometry at 260 nm [23].

2.8. Evaluation of cytotoxic potential of liposomal formulations

The cytotoxic activity of the developed formulations was assessed in SK-MEL-28 human melanoma cells (ATCC, Manassas, VA, USA) using an MTT assay adapted from a previously reported protocol [24]. Cells were maintained in Dulbecco's Modified Eagle Medium (DMEM) supplemented with 10% fetal bovine serum (FBS) and 1% penicillin–streptomycin at 37 °C in a humidified atmosphere containing 5% CO_2. Once adequate confluence was achieved, the cells were detached by trypsinization, seeded into 96-well plates at a density of 1×10^4 cells per well, and incubated for 24 h to allow attachment.

After the attachment period, the culture medium was removed and the cells were rinsed with phosphate-buffered saline (PBS). The wells were then treated with free 5-FU, blank liposomes, or formulations F1–F4 in a final volume of 150 µL per well, while incomplete DMEM was used as the negative control. The cells were exposed to the treatments for 24 or 48 h. At the end of each

incubation period, the treatment medium was discarded, the wells were washed, and 150 µL of MTT solution (250 µg/mL) was added. Following a 4 h incubation, the MTT solution was removed and the resulting formazan crystals were dissolved in 200 µL of dimethyl sulfoxide (DMSO). The plates were gently shaken for 15 min to ensure complete solubilization, and absorbance was measured at 570 nm using a microplate reader. Cell viability was expressed relative to the untreated control, and IC_{50} values were derived from the corresponding concentration–response curves.

2.9. Statistics

Statistical analysis was conducted using Microsoft Excel 2010 and OriginPro 6.1. All quantitative data are presented as mean ± standard deviation (SD). Differences among the experimental groups were assessed by one-way analysis of variance (ANOVA), followed by Student's *t*-test for pairwise comparisons. A p-value < 0.01 was considered statistically significant.

3.0 Results and Discussion

3.1 Size and Zeta Potential Analysis

The physicochemical characteristics of the developed liposomal systems are presented in Table 2. All formulations exhibited vesicle dimensions within the nanometer range. The mean particle sizes of blank liposomes (BL), 5-FU-loaded liposomes (F1), and chitosan-coated 5-FU liposomes (F2) were 237 ± 8.3, 225 ± 11.2, and 263 ± 10.6 nm, respectively. Their corresponding polydispersity index (PDI) values were 0.45 ± 0.04, 0.43 ± 0.02, and 0.48 ± 0.03. Compared with BL, formulation F1 showed a modest reduction in vesicle size. This decrease may be associated with the presence of polysorbate 80, which can reduce interfacial tension and facilitate more efficient organization of the phospholipid components during vesicle formation, thereby favoring the production of smaller liposomal structures [25].

In contrast, the chitosan-coated 5-FU liposome formulation (F2) exhibited a notable increase in vesicle size relative to the uncoated F1 (Table 2; Figure 1). This enlargement is attributed to the formation of a chitosan layer on the vesicle surface via electrostatic interaction between the positively charged amino groups of chitosan and the negatively charged phospholipid head groups.

Zeta potential analysis further confirmed the surface modification, with uncoated liposomes (F1) showing a slightly negative potential (−5.8 ± 0.7 mV), whereas chitosan-coated 5-FU liposomes

(F2) exhibited a positive value (+15.7 ± 1.3 mV) due to the cationic nature of chitosan and its coating over the lipid vesicles. The charge reversal indicates successful adsorption of chitosan onto the liposome surface, forming a stable chitosan–liposome complex (chitosome) [26]. This modification enhances colloidal stability through increased electrostatic repulsion, thereby reducing the likelihood of particle aggregation. These observations are consistent with previous reports, which documented positive zeta potentials of approximately +19 mV for chitosan-coated 5-FU liposomes [27]. The increase in zeta potential in F2 is likely due to the higher chitosan adsorption on the negatively charged liposomal surface, confirming the effective surface functionalization [28] A uniformly distributed, stable, and stable vesicular system was confirmed by particle size, PDI and zeta potential measurements. The chitosan coating of liposomal formulation (F2) increased particle size and shifted the zeta potential, confirming successful surface modification. Neither F3 nor F4 had their dynamic light scattering parameters determined since liposomes were incorporated into the gel matrix, thereby transforming the system from a colloidal dispersion into a semisolid. The precursor formulations of F3 and F4 provide information about their vesicle characteristics.

3.4 Encapsulation Efficiency (EE%) and Drug Loading (DL%)

The 5-FU-loaded liposomes (F1), chitosan-coated 5-FU liposomes (F2), and 5-FU liposomal gel (F3) showed a stepwise increase in both entrapment efficiency (EE%) and drug loading (DL%). The EE% values increased from 48.67 ± 1.70% in F1 to 64.0 ± 2.16% in F2 and 78.33 ± 1.70% in F3, while the corresponding DL% values were 3.2 ± 0.08%, 5.1 ± 0.12%, and 6.3 ± 0.12%, respectively. A further improvement was observed for the chitosan-coated 5-FU liposomal gel (F4), which achieved an EE% of 81 ± 2.45% and a DL% of 9.2 ± 0.12%. These results suggest that both chitosan coating and incorporation into the gel matrix contributed to improved retention of 5-FU within the formulation. Similar observations have been reported for chitosan-coated liposomal systems, where adsorption of the polymer onto the vesicle surface may reduce drug leakage and enhance overall drug retention [29]. Because 5-FU is hydrophilic, it is expected to be predominantly associated with the aqueous compartment of the liposomes. The higher EE% and DL% observed after chitosan coating may therefore arise from additional drug–polymer interactions and the formation of a surface barrier that limits diffusion of 5-FU from the vesicles [16].

3.2 ATR-FTIR analysis

ATR-FTIR analysis was performed to identify the principal functional groups of the individual formulation components and to assess possible intermolecular interactions following liposome formation. Cholesterol displayed its main absorption bands in the aliphatic region, with signals at 2922.02 and 2853.22 cm^{-1} attributed to C–H stretching vibrations. Additional bands were detected at 1734.69 cm^{-1} and 1462.30 cm^{-1}, corresponding to carbonyl-related stretching and C–H deformation, respectively [10]. Signals appearing at lower wavenumbers, including 1375.8, 1161, 1115.3, and 721.7 cm^{-1}, were associated with bending, stretching, and rocking vibrations of the functional groups present within the cholesterol structure.

The soybean lecithin spectrum exhibited a comparable lipid-associated profile. Strong absorption bands occurred at 2923.4 and 2854.1 cm^{-1}, while another signal was observed at 3008.1 cm^{-1}. A prominent band at 1743.1 cm^{-1} was assigned to ester carbonyl stretching, consistent with the phospholipid structure. Further characteristic absorptions were identified at 1460.8 and 1375.5 cm^{-1}, whereas bands at 1160.5 and 721.7 cm^{-1} were detected in the fingerprint region [30]. The similarity between several cholesterol and lecithin bands reflects the predominance of hydrocarbon chains and lipid-associated functional groups in both components.

In contrast, chitosan exhibited a distinct spectral profile characteristic of a polysaccharide-based polymer. A broad absorption band centered at 3275.01 cm^{-1} was observed in the high-wavenumber region, together with a C–H stretching signal at 2906.4 cm^{-1}. The fingerprint region was dominated by a strong band at 1013.3 cm^{-1}, corresponding to C–O-containing groups within the polysaccharide backbone, while an additional low-frequency signal appeared at 531.4 cm^{-1} [31]. These characteristic bands confirmed the presence of the principal functional groups associated with the chitosan matrix. The spectrum of 5-fluorouracil (5-FU) was distinguishable from those of the lipid and polymeric components. Absorption bands at 2993.2 and 2826 cm^{-1} were recorded in the C–H stretching region, while a prominent signal at 1645.2 cm^{-1} was associated with unsaturated bond vibrations. Additional characteristic bands were observed at 1425, 1348, and 803.6 cm^{-1}, representing vibrations within the heterocyclic structure of 5-FU [32].

Following liposome formation, the resulting spectrum exhibited characteristic absorptions from both the lipid components and associated functional groups. Major bands were detected at 3306.5,

2979.8, and 1645.5 cm^{-1}, while additional signals appeared at 1085.2, 1044.2, 876.9, and 535.1 cm^{-1}. The retention of the principal characteristic bands without the appearance of major new absorption signals suggests that formulation development did not induce substantial chemical alteration of the incorporated components.

Comparison of the individual and formulated spectra therefore indicated satisfactory physicochemical compatibility among cholesterol, soybean lecithin, chitosan, and 5-FU. The close correspondence of the lipid-associated bands supports compatibility between cholesterol and lecithin within the vesicular bilayer. Meanwhile, modest changes in bands associated with hydroxyl, amino, and other polar groups may reflect non-covalent interactions involving chitosan, including hydrogen bonding and electrostatic association. The preservation of characteristic 5-FU signals within the formulated system further suggests that the drug remained chemically intact after incorporation. Overall, the ATR-FTIR findings support successful integration of 5-FU and chitosan into the liposomal system without evidence of major incompatibility or formation of new covalent species.

3.3 Surface Morphology of the prepared liposomes

The surface morphology of liposomal formulations is presented in Figure 3. The images revealed that the liposomes were uniformly distributed and exhibited a spherical shape. No aggregation was observed in any of the formulations, indicating good colloidal stability. The SEM images illustrate observable differences in the surface morphology of the formulations. Figure 3 (a) shows well-defined, spherical vesicles with relatively uniform size distribution, indicating the formation of 5-FU loaded liposomes (F1). In Figure 3 (b), the vesicles appear slightly larger with smoother and more defined boundaries, suggesting successful chitosan coating (F2), which may have contributed to improved structural integrity. In contrast, Figure 3 (c) exhibits an irregular and aggregated appearance with indistinct vesicular structures, likely due to the incorporation of liposomes into the gel matrix (F3), which conceals individual vesicles. Figure 3 (d) shows a more compact and homogeneous surface with reduced visible vesicular boundaries compared to 3 (c), indicating the formation of a chitosan-coated 5-FU liposomal gel (F4), where the combined effect of gel matrix and chitosan results in a denser and more uniform morphology.

3.5 Physical Stability Studies

Changes in vesicle size after one month of storage at 4 ± 1 °C and 25 ± 2 °C were used to assess the physical stability of the developed formulations (Figure 4). The uncoated liposomal formulation (F1) showed a modest increase in particle size during storage, whereas the blank liposomes exhibited a comparatively greater enlargement. This increase may be associated with aggregation or fusion of neighboring vesicles, which can occur because of the dynamic and flexible nature of phospholipid bilayers. Rearrangement of bilayer components, particularly in the presence of surfactants, may promote vesicle–vesicle interactions and consequently increase the apparent particle size. By comparison, chitosan-coated liposomes exhibited only limited changes in vesicle dimensions throughout the one-month storage period, indicating improved resistance to physical destabilization. The enhanced stability may be attributed to the formation of a chitosan layer around the negatively charged liposomal surface. This polymeric coating can provide an additional steric and electrostatic barrier against vesicle aggregation and fusion, thereby helping to preserve particle size during storage. Overall, the comparatively small size variation observed for the chitosan-coated system supports the stabilizing role of the surface polymeric layer
[33].

A 30-day assessment of liposomal formulations (F1-F4) under two storage conditions (4 ± 1 ℃ and 25 ± 2 °C with 60 % relative humidity) was conducted by investigating variations in entrapment efficiency (EE%), particle size and polydispersity index (PDI), as reported in Figure 4. The study showed that EE% decreased gradually in all formulations over the storage period, with a more pronounced decrease at 25 ± 2 °C in comparison to refrigerated storage (4 ± 1 °C). It was observed that entrapment in F1 at 4 ± 1 ℃ reduced from 48% to 38% whereas at 25 ± 2 °C reduced from 48% to 31% after 30 days. A higher EE retention was observed with F4 than all other formulations, with 64% EE retained at 4 ± 1 °C as opposed to 60% RH at 25 ± 2 °C. Low storage temperatures effectively reduce drug leakage, consequently preserving encapsulation effectiveness [34]. According to this results, phospholipid bilayer fluidity changes depending on temperature, and elevated temperatures lead to a greater permeability of the membrane and eventual drug leakage. In all formulations, vesicle diameter gradually increased during storage, indicating aggregation or fusion of liposomal vesicles [35]. Over 30 days, the blank liposomes (control) increased from 237 nm to 280 nm at 4 ± 1°C and from 237 nm to 284 nm at 25 ± 2 °C. Drug-loaded formulations showed a similar trend: F1 increased from 225 nm to 268 nm at 4 ± 1 °C and 274 nm at 25 ± 2 °C. At 25 ± 2 °C, the increase was more pronounced, suggesting that higher

storage temperatures speed up vesicle instability, fusion, or aggregation [36]. A significant increase in PDI values (from 0.43 to 0.69) was observed during the storage period. PDI increases as the size distribution increases, suggesting a loss of uniformity among vesicles. At 25 ± 2 °C, there was a more pronounced effect, which corresponds to the observed particle size growth and reduction in entrapment efficiency. PDI increases over time, leading to colloidal instability, and refrigerated storage provides better control over vesicle uniformity than ambient storage. As compared with room temperature storage, liposomal formulations kept better physical and colloidal stability when refrigerated [37]. F4 showed the greatest stability in terms of entrapment efficiency and size retention, likely due to its higher initial drug loading and compact bilayer arrangement compared to the other tested formulations. The results demonstrate the importance of temperature-controlled storage for prolonging the stability of liposomal formulations, since storage at 25 ± 2 °C resulted in accelerated drug leakage and particle growth, increased PDI and reduced entrapment efficiency.

3.6 Skin Irritancy Test

The skin biocompatibility of the developed liposomal formulations was evaluated using a rat ear model, with erythema and edema serving as primary indicators of irritation. As illustrated in Figure 5, all formulations exhibited minimal irritation compared to the standard irritant, formalin, which produced pronounced erythema and edema, thereby validating the sensitivity of the experimental model [38]. The control group containing 5-FU solution showed no signs of irritation (0.0 ± 0.0, not shown), indicating that the drug itself is not inherently irritating under the tested conditions. In contrast, the positive control (formalin) exhibited significantly higher edema (3.70 ± 0.39) and erythema (4.5 ± 0.35) scores. Among the liposomal formulations, edema scores were recorded as F1 (1.21 ± 0.14), F2 (1.43 ± 0.09), F3 (1.42 ± 0.05), and F4 (1.37 ± 0.27), while erythema scores were F1 (0.95 ± 0.11), F2 (0.99 ± 0.26), F3 (1.03 ± 0.42), and F4 (0.85 ± 0.15), respectively. All these values fall below the threshold score of 2, classifying the formulations as non-skin irritants [39]. Among the tested formulations, F4 demonstrated the lowest erythema and comparatively low edema scores, indicating superior skin compatibility. This enhanced tolerability can be attributed to the chitosan coating in the gel-based system, which likely provides a protective barrier, reduces direct drug-skin interaction, and promotes controlled drug release. Chitosan is well known for its biocompatibility and bioadhesive nature, contributing to reduced irritation and improved skin

retention. Although minor variations were observed among F1, F2, and F3, these differences were not significant and all formulations maintained a non-irritant profile. The slightly higher edema values in F2 and F3 may be related to formulation-specific factors such as lipid composition or vesicle characteristics, which can influence skin interaction.

All liposomal formulations (F1-F4) loaded with 5-FU showed minimal erythema and edema in the rat ear model over a 24-hour period. [38]. These findings confirm the favorable skin compatibility of the developed systems and support their potential application in transdermal or topical delivery of 5-FU.

3.7 *In vitro* 5-FU Release Studies

The release profiles of 5-FU varied markedly according to the type of delivery system employed (Figure 6). The free 5-FU solution exhibited the fastest release, with approximately two-thirds of the drug diffusing through the membrane within the first 30 min and essentially complete release occurring by 2 h. This rapid transport is consistent with the hydrophilic nature and relatively small molecular size of 5-FU, which allow the drug to diffuse readily in the absence of a carrier-mediated barrier.

A considerably slower release pattern was observed for the liposomal formulations. After 2 h, F1 and F2 released 30.4 ± 1.24% and 29.3 ± 1.50% of their 5-FU content, respectively. The cumulative release subsequently increased to 45.7 ± 1.76% for F1 and 52.2 ± 1.85% for F2 at 12 h. The fraction released during the early stage may originate mainly from non-entrapped drug or 5-FU located close to the vesicle surface, which can diffuse rapidly into the surrounding medium. Thereafter, drug release became more gradual as 5-FU associated with the internal aqueous phase had to traverse the lipid membrane before reaching the receptor medium. The phospholipid bilayer therefore functioned as a diffusional barrier, contributing to the prolonged release behavior observed for the liposomal systems [40]. Furthermore, liposomes are known to undergo structural and morphological adaptation, enabling them to maintain integrity while facilitating controlled drug transport across biological environments [41]. A further extension in drug release was observed for the chitosan-coated 5-FU liposomes (F2), where cumulative release at 12 h (52.2 ± 1.85%) was higher than F1 but still controlled. This behavior can be attributed to the chitosan coating, which enhances vesicle stability and prolongs drug retention by forming a polymeric barrier around the liposomes [42]. The gel-based formulations (F3 and F4) exhibited

comparatively higher cumulative release but maintained a controlled diffusion pattern. Within the first 4 h, F3 and F4 released 41.2 ± 1.36% and 48.3 ± 1.87% of 5-FU, respectively. At 12 h, cumulative release increased to 68.21 ± 1.99% for F3 and 74.3 ± 2.15% for F4. After 24 h, the total drug release was recorded as 75.7 ± 1.86% for F3 and 79.6 ± 1.33% for F4, whereas F1 and F2 showed comparatively lower release values of 61.4 ± 1.30% and 63.2 ± 1.54%, respectively. The higher release from gel formulations can be attributed to improved hydration and swelling of the gel matrix, which facilitates drug diffusion. Notably, F4 (chitosan-coated 5-FU liposomal gel) exhibited the highest cumulative release (79.6 ± 1.33%) among all formulations, while still maintaining a sustained release pattern. The relatively slower release rate compared to the aqueous solution, despite higher cumulative release, indicates effective modulation of drug diffusion. The attenuated release kinetics of chitosan-modified systems are attributed to the presence of a polymeric diffusion barrier that restricts drug release into the surrounding medium [43]. The formulations exhibited a two-stage release behavior over the 24 h study period. A relatively rapid liberation of 5-FU occurred initially, most likely reflecting the diffusion of non-entrapped drug and molecules loosely associated with the vesicular surface. This was followed by a slower release phase, during which transport of 5-FU was progressively restricted by the lipid membrane and, in chitosan-containing systems, by the additional polymeric barrier. These diffusional constraints contributed to the prolonged release of the drug throughout the experimental period [44].

3.8 Release Kinetics

Table 3 summarizes the kinetic modeling of 5-FU release from F1, F2, F3, and F4. Among the investigated models, the Higuchi equation provided the closest fit, with R^2 values between 0.910 and 0.981, suggesting that diffusion was the predominant mechanism governing drug release from the formulations. The gel-based systems, F3 and F4, also showed comparatively high agreement with the Hixson–Crowell model, with R^2 values of 0.885 and 0.895, respectively. This finding indicates that, in addition to diffusion, changes in matrix dimensions or surface characteristics may have contributed to the release process.

Interpretation of the Korsmeyer–Peppas exponent further supported the diffusion-controlled behavior. In general, an exponent value of $n \leq 0.5$ is associated with Fickian diffusion, whereas values between 0.5 and 1.0 indicate anomalous or non-Fickian transport. An n value of 1.0 corresponds to Case II transport, while values above 1.0 are indicative of Super Case II transport

[45]. For the chitosan-coated 5-FU liposomal gel, the calculated *n* value was 0.312, confirming a predominantly Fickian diffusion mechanism. Collectively, the kinetic findings indicate that the liposomal systems were capable of restricting rapid drug liberation and maintaining 5-FU release over an extended period [45].

3.9 *Ex Vivo* Skin Permeation of the Drug

Figure 7 presents the 24 h transdermal permeation profiles of 5-FU through excised rat skin using Franz diffusion cells containing phosphate-buffered saline (pH 7.4) as the receptor medium. Free 5-FU showed minimal transport across the skin barrier, with only 8.2 ± 1.66% permeating after 24 h, highlighting the limited skin permeability of the hydrophilic drug in solution form. Incorporation into liposomal carriers markedly increased 5-FU permeation. Formulation F1 achieved a cumulative permeation of 43.7 ± 1.05%, substantially exceeding that of the free drug. This improvement may be related to the nanoscale dimensions of the vesicles and the interaction of their lipid components with the stratum corneum, which can facilitate drug partitioning and subsequent diffusion across the skin [46]. The relatively small vesicle size may also improve contact with the skin surface and increase the effective area available for drug transport [6]. A further increase in permeation was observed with the chitosan-coated formulation F2, which reached 61.37 ± 1.47% after 24 h. The enhanced performance of F2 may be associated with the presence of the chitosan surface layer, which can strengthen interactions between the formulation and the skin surface and prolong local residence. These interactions may facilitate closer vesicle–skin contact and contribute to the greater transdermal transport of 5-FU compared with the uncoated liposomal formulation.

Among the gel-based formulations, F3 produced a cumulative 5-FU permeation of 55.35 ± 1.12% after 24 h. This value exceeded that of F1 but remained lower than those obtained with the chitosan-containing systems, F2 and F4. Incorporation of the liposomal dispersion into the gel matrix may have improved formulation retention and contact with the skin surface, although the higher viscosity of the gel could also have slowed drug diffusion. Accordingly, permeation from F3 likely reflected a balance between improved surface residence and viscosity-mediated resistance to drug transport [47]. The greatest permeation was observed with F4, which reached 73.7 ± 1.44% at 24 h. This enhanced performance may result from the combined contribution of liposomal encapsulation, chitosan surface modification, and prolonged residence provided by the

gel vehicle. Although the gel matrix can limit rapid diffusion, it may simultaneously support a more sustained concentration gradient at the skin surface, thereby favoring prolonged topical delivery [48]. Both chitosan-containing formulations, F2 and F4, showed significantly greater permeation than their corresponding uncoated systems, F1 and F3 ($p < 0.05$), supporting the contribution of chitosan to enhanced skin transport. Tween 80 may have provided an additional permeation-enhancing effect by interacting with stratum corneum components and altering lipid organization within the skin barrier. Such surfactant-mediated changes can increase membrane fluidity and reduce resistance to drug diffusion, thereby facilitating transdermal transport [25]. The extent of this effect is largely determined by the ability of the surfactant to modify or fluidize intercellular lipid domains within the stratum corneum [6].

3.10 Skin Drug Retention

Figure 8 presents the estimated retention of 5-FU within the skin after 24 h of exposure. Compared with free 5-FU dispersed in phosphate-buffered saline (PBS), all liposomal formulations produced greater cutaneous drug deposition. The retained drug fractions were 5.8 ± 1.02% for F1, 7.3 ± 1.13% for F2, 6.5 ± 1.01% for F3, and 9.3 ± 1.07% for F4. Among the investigated systems, the chitosan-coated 5-FU liposomal gel (F4) showed the greatest skin retention, indicating a stronger capacity to maintain the drug within the cutaneous tissue. The higher deposition observed with F4 may be associated with the combined influence of vesicle size, chitosan coating, and the presence of Tween 80, which can enhance interaction of the formulation with the skin barrier and facilitate drug partitioning into cutaneous layers [49]. Differences in particle size may also affect the extent and depth of drug accumulation within the skin. Nevertheless, the exact contribution of each formulation factor to the enhanced retention cannot be determined from the present data alone, and further mechanistic studies would be required to clarify the pathways responsible for 5-FU deposition in the skin.

3.11 The Physicochemical Characterization of the Skin

The ATR-FTIR spectra of the excised skin obtained after the permeation experiment were evaluated to identify formulation-induced changes in the molecular organization of the cutaneous barrier. Compared with untreated skin, most formulations produced shifts in characteristic bands associated with lipid and protein components, suggesting alterations in stratum corneum

organization that may have facilitated 5-FU transport and retention. In the epidermal region, prominent bands were initially detected near 3300, 2922, and 2850 cm^{-1}. Following treatment with the liposomal formulations, particularly F2 and F3, these signals shifted toward higher wavenumbers, as shown in Figure 10. The displacement of the broad band around 3300 cm^{-1} to approximately 3316.0 cm^{-1} may reflect changes in hydrogen-bonding environments involving O–H and N–H groups associated with skin proteins and polar lipid components. Changes were also observed in the dermal spectra, where a shift from approximately 3296 to 3318.1 cm^{-1} was detected, further indicating modification of the local molecular environment [50]. In addition, bands within the 2850–2920 cm^{-1} region, which are commonly associated with CH_2 stretching vibrations of lipid hydrocarbon chains and protein-associated structures, were altered following treatment with F2 and F3, as illustrated in Figure 9.

4.12 *In vitro* cellular cycle analysis

4.12.1 Evaluation of Cellular Toxicity

The cytotoxic activity of blank liposomes (BL), free 5-FU, and formulations F1–F4 was assessed in SK-MEL-28 melanoma cells using the MTT assay. A clear formulation- and time-dependent increase in cytotoxicity was observed. Among the tested systems, F4 produced the strongest growth-inhibitory effect, followed by F3, F2, and F1, whereas free 5-FU required comparatively higher concentrations to achieve a similar reduction in cell viability. After 48 h of exposure, F4 suppressed melanoma cell growth by approximately 94%, indicating the greatest antiproliferative activity among the investigated formulations. This trend was further supported by the IC_{50} values. At 24 h, the IC_{50} values for BL, free 5-FU, F1, F2, F3, and F4 were 100, 0.59, 0.51, 0.31, 0.23, and 0.18 µg/mL, respectively. After 48 h, these values decreased to 50, 0.09, 0.08, 0.06, 0.05, and 0.03 µg/mL, respectively, demonstrating greater cytotoxic activity with prolonged exposure. The markedly lower IC_{50} of F4 suggests that incorporation of 5-FU into the chitosan-coated liposomal gel enhanced its anticancer effect against SK-MEL-28 cells. This improvement may be related to enhanced cellular interaction and drug delivery provided by the liposomal carrier and chitosan coating. In addition, chitosan itself has been reported to exhibit anticancer-related biological activity, which may have contributed to the overall cytotoxic response.

4.0 Conclusion

The present study successfully developed and characterized 5-FU-loaded liposomal formulations and their chitosan-coated counterparts for topical melanoma therapy. Chitosan surface modification improved formulation stability, prolonged drug release, and enhanced cutaneous retention compared with uncoated liposomes. Collectively, these findings indicate that the developed vesicular systems can facilitate sustained delivery of 5-FU across the skin and may improve its local availability at the target site. The results therefore highlight the potential of lipid–polymer hybrid carriers as promising platforms for controlled topical drug delivery. Nevertheless, further *in vivo* investigations are required to confirm their therapeutic efficacy, safety, pharmacokinetic behavior, and long-term tolerability. Future development may also focus on incorporating targeting moieties or stimuli-responsive components to further improve site-specific delivery and therapeutic performance in melanoma treatment.

Acknowledgements:

The authors wish to thank Faculty of Pharmacy Gomal University; Faculty of Pharmacy, Universiti Malaya; Faculty of Pharmacy, Universiti Sultan Zainal Abidin (UniSZA) and Faculty of Pharamcy, Universiti Teknologi MARA (UiTM) for their support.

Funding Sources:

This research received no external funding.

Disclosure of Potential Conflicts of Interest

The authors declare no conflicts of interest.

Research Involving Human Participants and/or Animals

This study did not involve human participants. All animal-related procedures, including the dermal irritation and *ex vivo* skin permeation experiments, were reviewed and approved by the Ethics Review Board of Gomal University, Dera Ismail Khan, Khyber Pakhtunkhwa, Pakistan (Ethical Approval No. 518/ERB/GU). The animal experiments were performed in accordance with institutional guidelines for the care and use of laboratory animals, and the study was reported in compliance with the ARRIVE guidelines.

References

[1] A. H. Roky, M. M. Islam, A. M. F. Ahasan, M. S. Mostaq, M. Z. Mahmud, M. N. Amin*, et al.*, "Overview of skin cancer types and prevalence rates across continents," *Cancer pathogenesis and therapy,* vol. 3, pp. 89-100, 2025.

[2] Z. Wang, B. Zhai, J. Sun, X. Zhang, J. Zou, Y. Shi*, et al.*, "Recent advances of injectable in situ-forming hydrogels for preventing postoperative tumor recurrence," *Drug delivery,* vol. 31, p. 2400476, 2024.

[3] A. Verma, K. Patel, and A. Kumar, "Targeting drug resistance in breast cancer: the potential of miRNA and nanotechnology-driven delivery systems," *Nanoscale Advances,* vol. 6, pp. 6079-6095, 2024.

[4] R. Neupane, S. H. Boddu, M. S. Abou-Dahech, R. D. Bachu, D. Terrero, R. J. Babu*, et al.*, "Transdermal delivery of chemotherapeutics: Strategies, requirements, and opportunities," *Pharmaceutics,* vol. 13, p. 960, 2021.

[5] L. M. Makha, "Design and synthesis of a nanocapsule system for transdermal delivery of lignocaine across the skin," 2024.

[6] Y.-Q. Yu, X. Yang, X.-F. Wu, and Y.-B. Fan, "Enhancing permeation of drug molecules across the skin via delivery in nanocarriers: novel strategies for effective transdermal applications," *Frontiers in bioengineering and biotechnology,* vol. 9, p. 646554, 2021.

[7] M. Adnan, M. H. Akhter, O. Afzal, A. S. Altamimi, I. Ahmad, M. A. Alossaimi*, et al.*, "Exploring nanocarriers as treatment modalities for skin cancer," *Molecules,* vol. 28, p. 5905, 2023.

[8] H. Nsairat, D. Khater, U. Sayed, F. Odeh, A. Al Bawab, and W. Alshaer, "Liposomes: Structure, composition, types, and clinical applications," *Heliyon,* vol. 8, 2022.

[9] A. Zafar, K. N. Alruwaili, S. K. Alharbi, H. N. Alotaibi, and M. Jafar, "Liposome preparation and related techniques," *Liposomes for Functional Foods and Nutraceuticals,* pp. 41-64, 2022.

[10] R. Gil-Gonzalo, D. A. Durante-Salmerón, S. Pouri, E. Doncel-Pérez, A. R. Alcántara, I. Aranaz*, et al.*, "Chitosan-coated liposome formulations for encapsulation of ciprofloxacin and etoposide," *Pharmaceutics,* vol. 16, p. 1036, 2024.

[11] C. Sebaaly, A. Trifan, E. Sieniawska, and H. Greige-Gerges, "Chitosan-coating effect on the characteristics of liposomes: A focus on bioactive compounds and essential oils: A review," *Processes,* vol. 9, p. 445, 2021.

[12] M. El-Tanani, S. M. Satyam, S. A. Rabbani, Y. El-Tanani, A. A. Aljabali, I. Al Faouri*, et al.*, "Revolutionizing Drug Delivery: The Impact of Advanced Materials Science and Technology on Precision Medicine," *Pharmaceutics,* vol. 17, p. 375, 2025.

[13] Y. Cao, X. Dong, and X. Chen, "Polymer-modified liposomes for drug delivery: from fundamentals to applications," *Pharmaceutics,* vol. 14, p. 778, 2022.

[14] A. Harugade, A. P. Sherje, and A. Pethe, "Chitosan: A review on properties, biological activities and recent progress in biomedical applications," *Reactive and Functional Polymers,* vol. 191, p. 105634, 2023.

[15] S. S. Imam, S. Alshehri, M. A. Altamimi, A. Hussain, W. Qamar, S. J. Gilani*, et al.*, "Formulation of piperine–chitosan-coated liposomes: Characterization and in vitro cytotoxic evaluation," *Molecules,* vol. 26, p. 3281, 2021.

[16] A. M. Yosef, R. S. Alqarni, F. Y. Sayd, M. S. Alhawiti, R. M. Almahlawi, K. Prabahar*, et al.*, "Preparation and characterization of novel polyelectrolyte liposomes using chitosan succinate layered over Chitosomes: a potential strategy for colon cancer treatment," *Biomedicines,* vol. 12, p. 126, 2024.

[17] M. M. Mady, M. M. Darwish, S. Khalil, and W. M. Khalil, "Biophysical studies on chitosan-coated liposomes," *European Biophysics Journal,* vol. 38, pp. 1127-1133, 2009.

[18] A. Alomrani, M. Badran, G. I. Harisa, M. ALshehry, M. Alhariri, A. Alshamsan*, et al.*, "The use of chitosan-coated flexible liposomes as a remarkable carrier to enhance the antitumor efficacy of 5-fluorouracil against colorectal cancer," *Saudi pharmaceutical journal,* vol. 27, pp. 603-611, 2019.

[19] Q. Wang, S. Lv, J. Lu, S. Jiang, and L. Lin, "Characterization, stability, and in vitro release evaluation of carboxymethyl chitosan coated liposomes containing fish oil," *Journal of food science,* vol. 80, pp. C1460-C1467, 2015.

[20] Z. Asghar, T. Jamshaid, U. Jamshaid, A. Madni, N. Akhtar, M. O. Lashkar*, et al.*, "In vivo evaluation of miconazole-nitrate-loaded transethosomal gel using a rat model infected with Candida albicans," *Pharmaceuticals,* vol. 17, p. 546, 2024.

[21] M. S. Latif, A. Nawaz, M. Asmari, J. Uddin, H. Ullah, and S. Ahmad, "Formulation development and in vitro/in vivo characterization of methotrexate-loaded nanoemulsion gel formulations for enhanced topical delivery," *Gels,* vol. 9, p. 3, 2022.

[22] M. A. Altamimi, A. Hussain, W. A. Mahdi, S. S. Imam, M. A. Alshammari, S. Alshehri*, et al.*, "Mechanistic insights into luteolin-loaded elastic liposomes for transdermal delivery: HSPiP predictive parameters and instrument-based evidence," *ACS omega,* vol. 7, pp. 48202-48214, 2022.

[23] A. Ali, A. Madni, H. Shah, T. Jamshaid, N. Jan, S. Khan*, et al.*, "Solid lipid-based nanoparticulate system for sustained release and enhanced in-vitro cytotoxic effect of 5-fluorouracil on skin Melanoma and squamous cell carcinoma," *Plos one,* vol. 18, p. e0281004, 2023.

[24] A. Nawaz and T. W. Wong, "Chitosan-carboxymethyl-5-fluorouracil-folate conjugate particles: Microwave modulated uptake by skin and melanoma cells," *Journal of Investigative Dermatology,* vol. 138, pp. 2412-2422, 2018.

[25] R. Bnyan, I. Khan, T. Ehtezazi, I. Saleem, S. Gordon, F. O'Neill*, et al.*, "Surfactant effects on lipid-based vesicles properties," *Journal of pharmaceutical sciences,* vol. 107, pp. 1237-1246, 2018.

[26] S. Gao, X. Yi, X. Gao, Z. Long, J. Guo, G. Xia*, et al.*, "Stabilization of β-Carotene Liposomes with Chitosan–Lactoferrin Coating System: Vesicle Properties and Anti-Inflammatory In Vitro Studies," *Foods,* vol. 14, p. 968, 2025.

[27] J. M. Joy, P. Amruth, P. K. Dara, V. Renuka, and R. Anandan, "Liposome mediated encapsulation and role of chitosan on modulating liposomal stability to deliver potential bioactives-A review," *Food Hydrocolloids for Health,* vol. 4, p. 100142, 2023.

[28] M. M. Badran, A. H. Alomrani, A. Almomen, Y. A. Bin Jardan, and A. E. S. Abou El Ela, "Novel metoprolol-loaded chitosan-coated deformable liposomes in thermosensitive in situ gels for the management of glaucoma: a repurposing approach," *Gels,* vol. 8, p. 635, 2022.

[29] I. Katouzian and R. A. Taheri, "Preparation, characterization and release behavior of chitosan-coated nanoliposomes (chitosomes) containing olive leaf extract optimized by response surface methodology," *Journal of food science and technology,* vol. 58, pp. 3430-3443, 2021.

[30] S. Betelu, I. Tijunelyte, L. Boubekeur Lecaque, I. Ignatiadis, A. Schnepf, E. Guenin*, et al.*, "Raman characterization of Phenyl-Derivatives: From primary amine to diazonium salts," *Journal of Organic & Inorganic Chemistry,* vol. 3, pp. 1-10, 2017.

[31] F. Mirzaee Rad, F. Tafvizi, H. Noorbazargan, and A. Iranbakhsh, "Ag-doped ZnO nanoparticles synthesized through green method using Artemisia turcomanica extract induce cytotoxicity and apoptotic activities against AGS cancer cells: an in vitro study," *Journal of Nanostructure in Chemistry,* vol. 14, pp. 403-418, 2024.

[32] H. E. Salama, G. R. Saad, and M. W. Sabaa, "Synthesis, characterization and biological activity of Schiff bases based on chitosan and arylpyrazole moiety," *International journal of biological macromolecules,* vol. 79, pp. 996-1003, 2015.

[33] X. Tan, Y. Liu, X. Wu, M. Geng, and F. Teng, "Layer-by-layer self-assembled liposomes prepared using sodium alginate and chitosan: Insights into vesicle characteristics and physicochemical stability," *Food Hydrocolloids,* vol. 149, p. 109606, 2024.

[34] M. A. Rahim, H. A. Zahran, H. M. Jaffar, S. Ambreen, M. F. Ramadan, F. Al-Asmari*, et al.*, "Liposomal encapsulation in food systems: A review of formulation, processing, and applications," *Food Science & Nutrition,* vol. 13, p. e70587, 2025.

[35] F. Song, G. Yang, Y. Wang, and S. Tian, "Effect of phospholipids on membrane characteristics and storage stability of liposomes," *Innovative Food Science & Emerging Technologies,* vol. 81, p. 103155, 2022.

[36] J. Y. Yu, P. Chuesiang, G. H. Shin, and H. J. Park, "Post-processing techniques for the improvement of liposome stability," *Pharmaceutics,* vol. 13, p. 1023, 2021.

[37] G. Amoabediny, F. Haghiralsadat, S. Naderinezhad, M. N. Helder, E. Akhoundi Kharanaghi, J. Mohammadnejad Arough*, et al.*, "Overview of preparation methods of polymeric and lipid-based (niosome, solid lipid, liposome) nanoparticles: A comprehensive review," *International Journal of Polymeric Materials and Polymeric Biomaterials,* vol. 67, pp. 383-400, 2018.

[38] M. Martins, F. Veiga, A. C. Paiva-Santos, and P. C. Pires, "Drug Repurposing and Nanotechnology for Topical Skin Cancer Treatment: Redirecting toward Targeted and Synergistic Antitumor Effects," *ACS Pharmacology & Translational Science,* vol. 8, pp. 308-338, 2025.

[39] S. Jahan, N. Sultana, A. Ali, N. A. Emad, P. Alam, M. Mujeeb*, et al.*, "5-Fluorouracil-and Sesamol-Loaded Transliposomal Gel for Skin Cancer: In Vitro, Ex Vivo, and Dermatokinetic Evaluation," *ACS omega,* vol. 10, pp. 6857-6875, 2025.

[40] Z. Izadiyan, M. Misran, K. Kalantari, T. J. Webster, P. Kia, N. A. Basrowi*, et al.*, "Advancements in Liposomal Nanomedicines: Innovative Formulations, Therapeutic Applications, and Future Directions in Precision Medicine," *International Journal of Nanomedicine,* pp. 1213-1262, 2025.

[41] S. Paramshetti, M. Angolkar, S. Talath, R. A. M. Osmani, A. Spandana, A. Al Fatease*, et al.*, "Unravelling the in vivo dynamics of liposomes: Insights into biodistribution and cellular membrane interactions," *Life Sciences,* p. 122616, 2024.

[42] W.-T. Chen, Y.-L. Kuo, C.-H. Chen, H.-T. Wu, H.-W. Chen, and W.-P. Fang, "Improving the stability and bioactivity of curcumin using chitosan-coated liposomes through a combination mode of high-pressure processing," *Lwt,* vol. 168, p. 113946, 2022.

[43] H. Chen, H. Pan, P. Li, H. Wang, X. Wang, W. Pan*, et al.*, "The potential use of novel chitosan-coated deformable liposomes in an ocular drug delivery system," *Colloids and surfaces B: biointerfaces,* vol. 143, pp. 455-462, 2016.

[44] E. G. Komarova, E. I. Senkina, A. S. Lozhkomoev, E. A. Kazantseva, K. A. Prosolov, S. O. Kazantsev*, et al.*, "Controlled anticancer 5-Fluorouracil release from functionalized 5-FU/PLGA/CaP coating on titanium implants: Characterization, in vitro drug delivery and cytotoxicity," *Materials Today Communications,* vol. 39, p. 109332, 2024.

[45] V. S. Shenoy, R. P. Gude, and R. S. R. Murthy, "In vitro anticancer evaluation of 5-fluorouracil lipid nanoparticles using B16F10 melanoma cell lines," *International nano letters,* vol. 3, p. 36, 2013.

[46] M. H. Abdallah, A. S. Abu Lila, H. M. El-Nahas, and T. M. Ibrahim, "Optimization of potential nanoemulgels for boosting transdermal glimepiride delivery and upgrading its anti-diabetic activity," *Gels,* vol. 9, p. 494, 2023.

[47] M. Pandey, H. Choudhury, B. Gorain, S. Q. Tiong, G. Y. S. Wong, K. X. Chan*, et al.*, "Site-specific vesicular drug delivery system for skin cancer: a novel approach for targeting," *Gels,* vol. 7, p. 218, 2021.

[48] S. Princely and M. Dhanaraju, "Design, formulation, and characterization of liposomal-encapsulated gel for transdermal delivery of fluconazole," *Asian J Pharm Clin Res,* vol. 11, pp. 417-424, 2018.

[49] O. Sarheed, M. Dibi, and K. V. Ramesh, "Studies on the effect of oil and surfactant on the formation of alginate-based O/W lidocaine nanocarriers using nanoemulsion template," *Pharmaceutics,* vol. 12, p. 1223, 2020.

[50] S. Azeez and R. Shenbagaraman, "Fourier transform infrared spectroscopy in characterization of bionanocomposites," in *Characterization Techniques in Bionanocomposites*, ed: Elsevier, 2025, pp. 209-227.

Table 1: The Composition of 5-Fluorouracil (5-FU)-Loaded Liposomes, Chitosan-Coated Liposomes, and Liposomal Gel Formulations.

Ingredients	Blank Formulation	F1(L)	F2 (CCL)	F3 (LG)	F4 (CCLG)
Soybean Lecithin (% w/w)	9	9	9	9	9
Cholesterol (% w/w**)**	1	1	1	1	1
5-FU (% w/w**)**	-	1	1	1	1
Chitosan (% w/w**)**	-	-	0.6	-	0.6
Tween 80 (% w/w**)**	-	0.2	0.2	0.2	0.2
Carbopol 940 (% w/w**)**	-	-	-	1	1
Triethanolamine (% w/w**)**	-	-	-	0.5	0.5
Buffer (ml)	20	20	20	-	-
Chloroform (q.s.)	(q.s.)	(q.s.)	(q.s.)	-	-

Note: Liposomes were prepared by molar ratios.
F1 (L): 5-FU-loaded liposomes; F2 (CCL): Chitosan-coated 5-FU liposomes; F3 (LG): 5-FU liposomal gel; F4 (CCLG): Chitosan-coated 5-FU liposomal gel.

Table 2: The physicochemical characteristics of Liposomal Formulations**.**

Formulation	Particle Size (nm)	Zeta Potential (mV)	PDI	Drug Loading (%)	%EE
BL	237 ± 8.30	-8.3 ± 0.50	0.45 ± 0.04	**--**	**---**
F1	225 ± 11.20	-5.8 ± 0.70	0.43 ± 0.02	3.2 ± 0.08	48.6 ± 1.70
F2	263 ± 10.60	15.7 ± 1.30	0.48 ± 0.03	5.1± 0.12	64.0 ± 2.16
F3	ND*	ND*	ND*	6.3 ± 0.12	78.3 ± 1.70
F4	ND*	ND*	ND*	9.2 ± 0.12	81.0 ± 2.45

ND: Not Determined

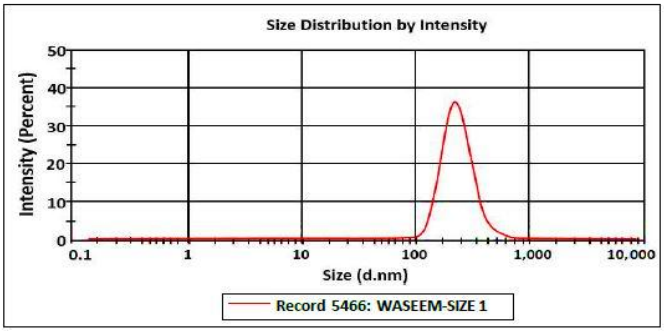
Table 3: *In vitro* drug release data fitted to various kinetic models for 5-FU loaded liposomes, chitosan-coated 5-FU liposome, 5-FU liposomal gel and chitosan-coated 5-FU liposomal gel. Correlation coefficients (R^2) of (F1–F4).

Formulation	Zero Order	First Order	Higuchi	Hixon	Korsmeyer-Peppas
F1	0.723	0.779	0.915	0.761	0.726
F2	0.835	0.896	0.975	0.761	0.803
F3	0.849	0.813	0.981	0.885	0.803
F4	0.839	0.820	0.978	0.895	0.804

(BL)

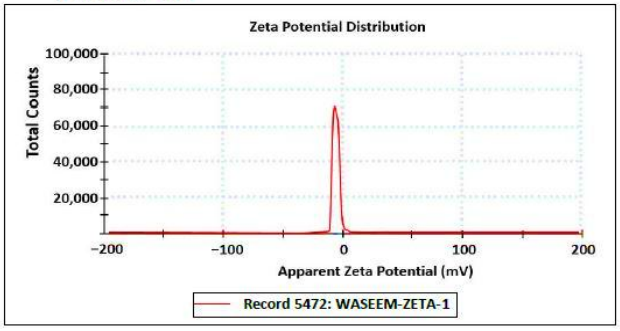
Results

		Size (d. nm):	% Intensity:	St Dev (d.n...
Z-Average (d. nm): 237.0	Peak 1:	259.1	96.6	23.01
PdI: 0.450	Peak 2:	0.000	0.0	0.000
Intercept: 0.956	Peak 3:	0.000	0.0	0.000
Result quality: Good				



Results

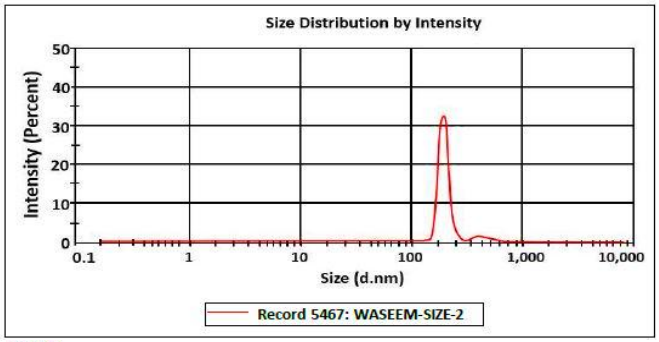
		Mean (mV)	Area (%)	St Dev (mV)
Zeta Potential (mV): -8.30	Peak 1:	-14.2	100.0	3.85
Zeta Deviation (mV): 3.85	Peak 2:	0.00	0.0	0.00
Conductivity (mS/cm): 0.114	Peak 3:	0.00	0.0	0.00
Result quality: Good				



(F1)

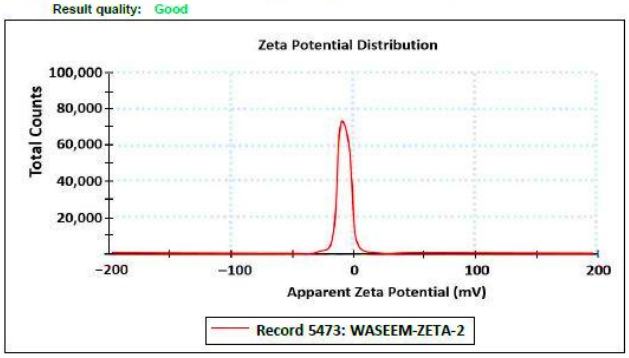
Results

		Size (d. nm):	% Intensity:	St Dev (d.n...
Z-Average (d. nm): 225.6	Peak 1:	241.9	98.3	51.20
PdI: 0.430	Peak 2:	458.2	4.4	2.450
Intercept: 0.958	Peak 3:	0.000	0.0	0.000
Result quality: Good				



Results

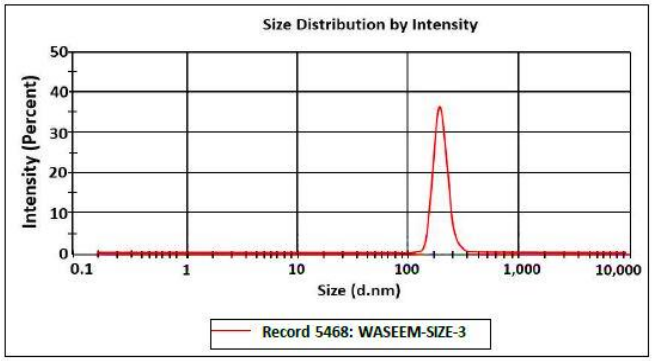
		Mean (mV)	Area (%)	St Dev (mV)
Zeta Potential (mV): -5.80	Peak 1:	-5.80	99.3	2.15
Zeta Deviation (mV): 2.15	Peak 2:	0.00	0.0	0.00
Conductivity (mS/cm): 0.119	Peak 3:	0.00	0.0	0.0
Result quality: Good				



(F2)

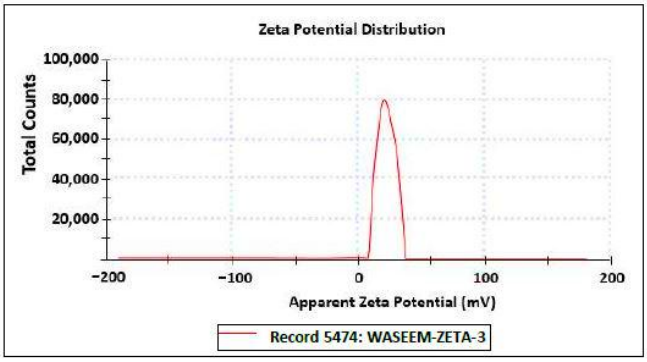
Results

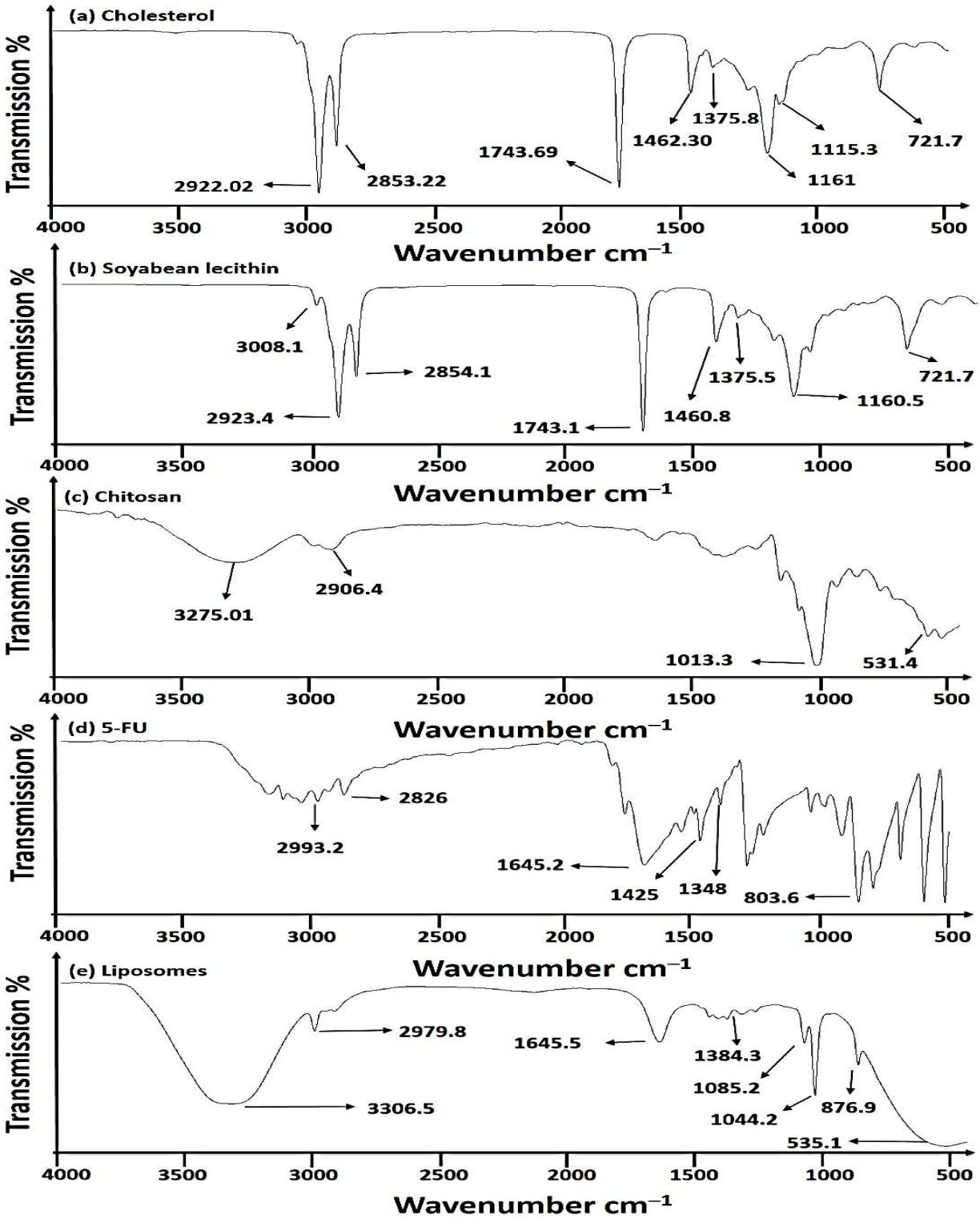
		Size (d. nm):	% Intensity:	St Dev (d.n...
Z-Average (d. nm): 263.4	Peak 1:	273.9	96.7	69.44
PdI: 0.480	Peak 2:	0.000	0.0	0.000
Intercept: 0.935	Peak 3:	0.000	0.0	0.000
Result quality: Good				

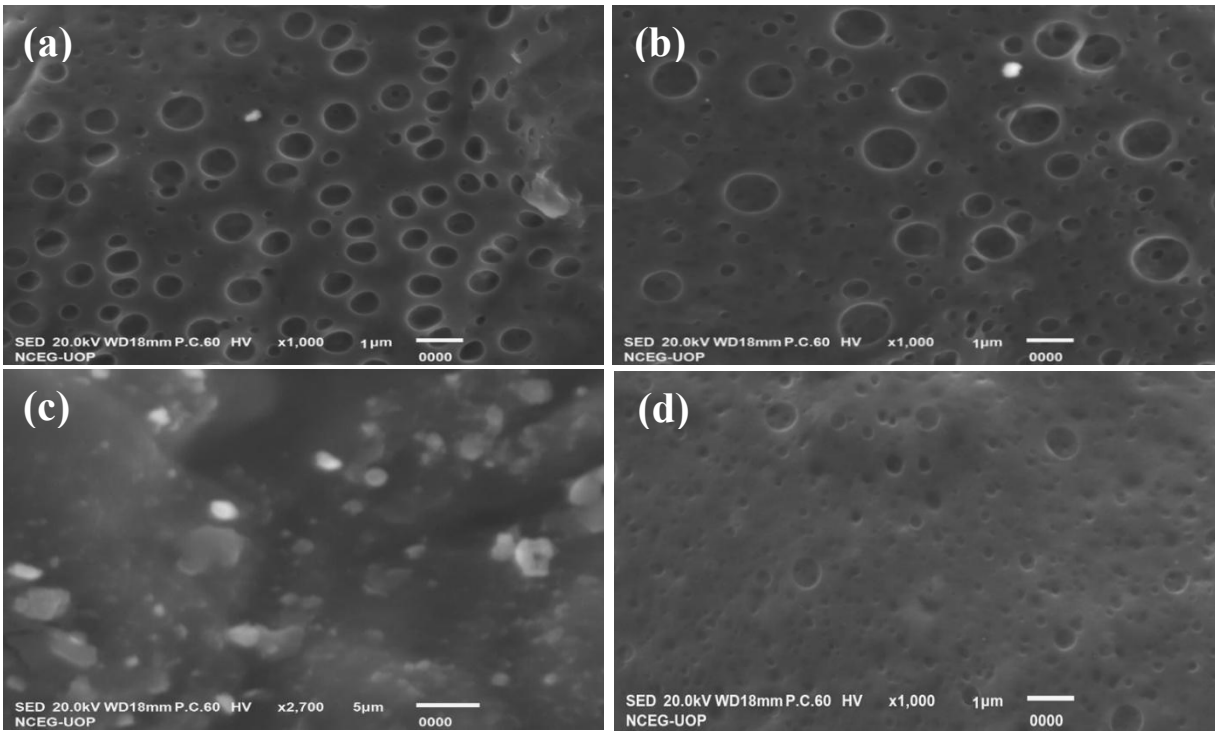


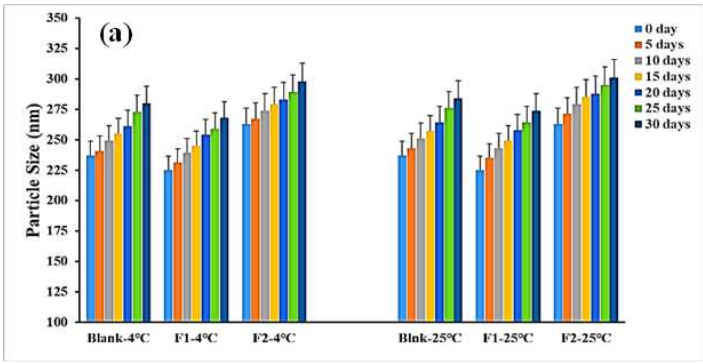
Results

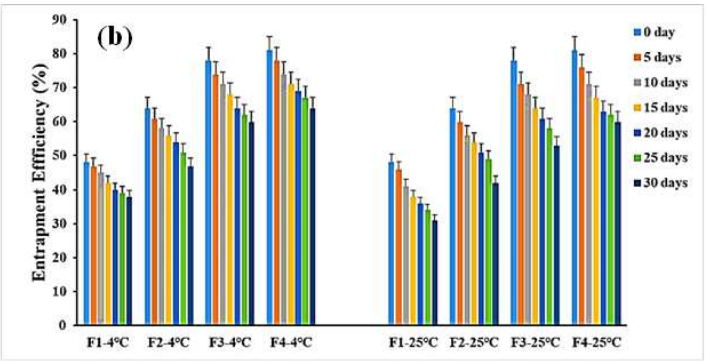
		Mean (mV)	Area (%)	St Dev (mV)
Zeta Potential (mV): 15.70	Peak 1:	22.8	99.3	4.36
Zeta Deviation (mV): 4.36	Peak 2:	0.00	0.0	0.00
Conductivity (mS/cm): 0.119	Peak 3:	0.00	0.0	0.00
Result quality: Good				

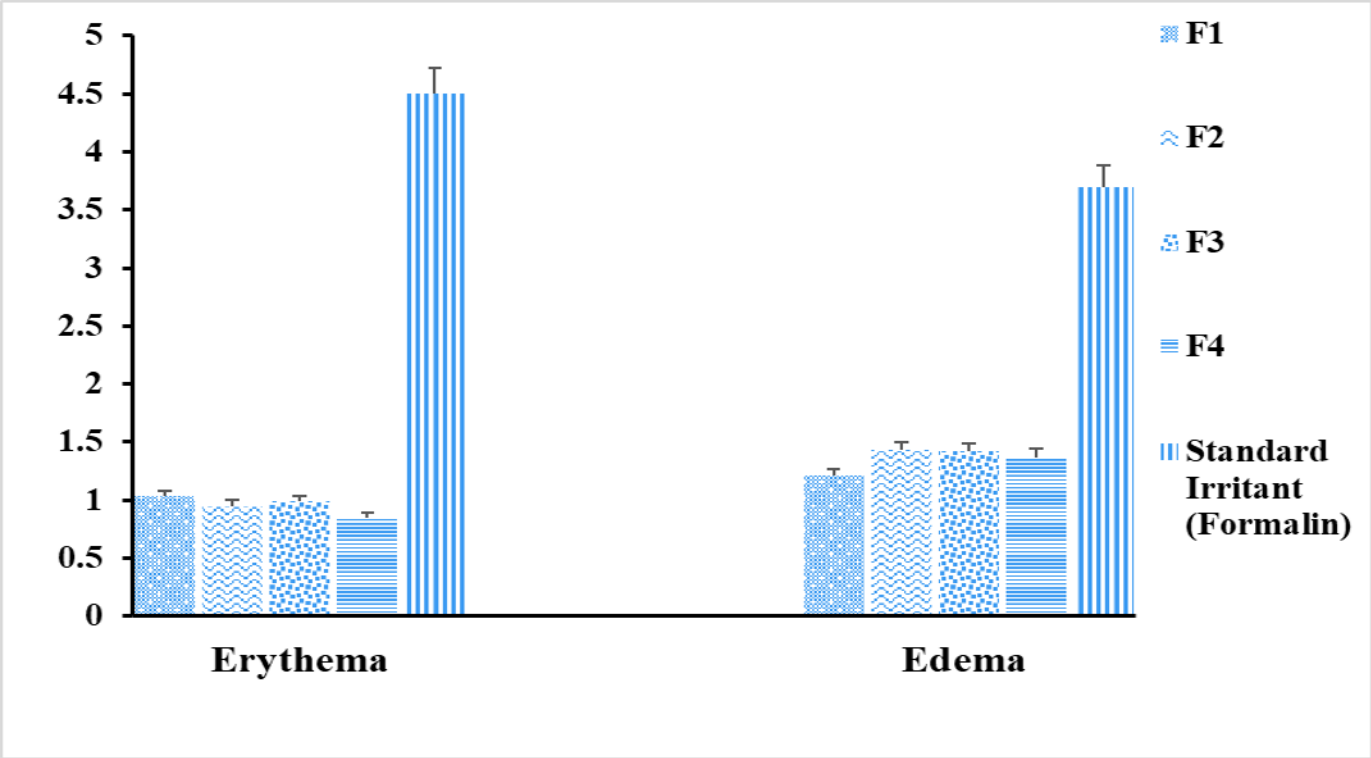


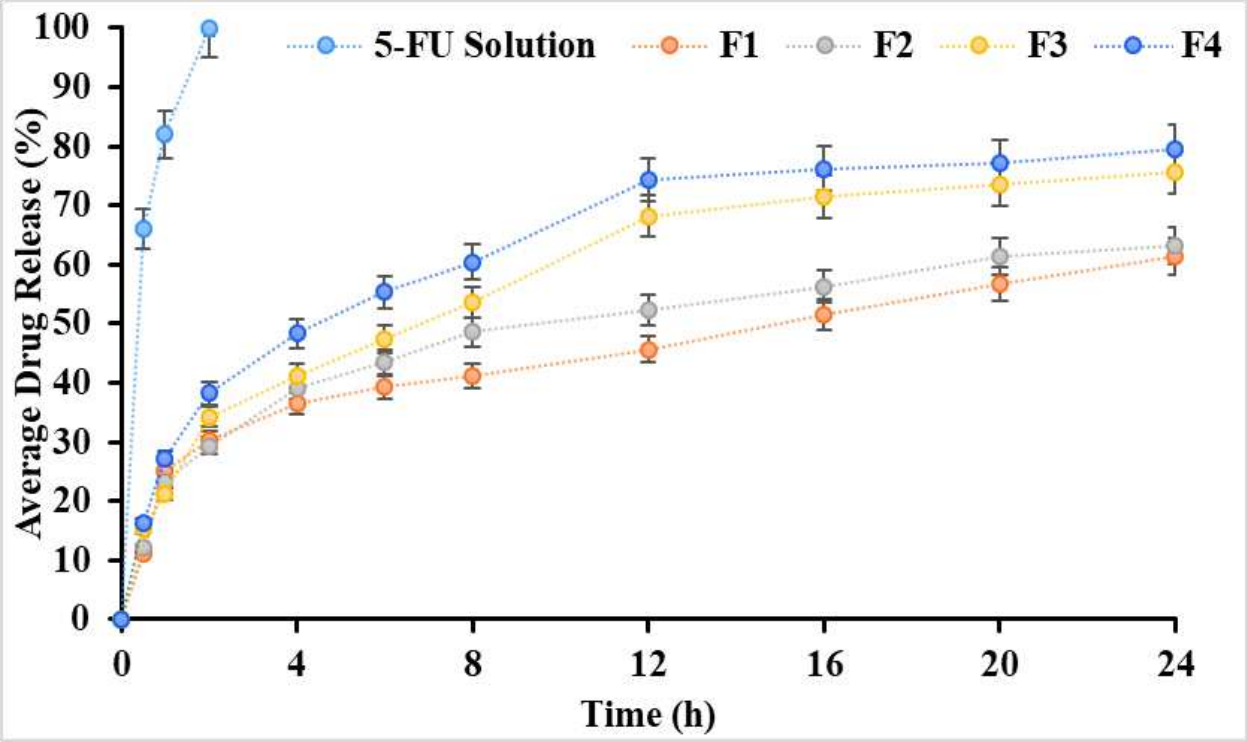

(a) Cholesterol
Transmission %
2922.02
2853.22
1743.69
1462.30
1375.8
1115.3
1161
721.7
4000
3500
3000
2500
2000
1500
1000
500
Wavenumber cm⁻¹
(b) Soyabean lecithin
Transmission %
3008.1
2854.1
2923.4
1743.1
1460.8
1375.5
1160.5
721.7
4000
3500
3000
2500
2000
1500
1000
500
Wavenumber cm⁻¹
(c) Chitosan
Transmission %
3275.01
2906.4
1013.3
531.4
4000
3500
3000
2500
2000
1500
1000
500
Wavenumber cm⁻¹
(d) 5-FU
Transmission %
2826
2993.2
1645.2
1425
1348
803.6
4000
3500
3000
2500
2000
1500
1000
500
Wavenumber cm⁻¹
(e) Liposomes
Transmission %
2979.8
1645.5
1384.3
1085.2
1044.2
876.9
3306.5
535.1
4000
3500
3000
2500
2000
1500
1000
500
Wavenumber cm⁻¹

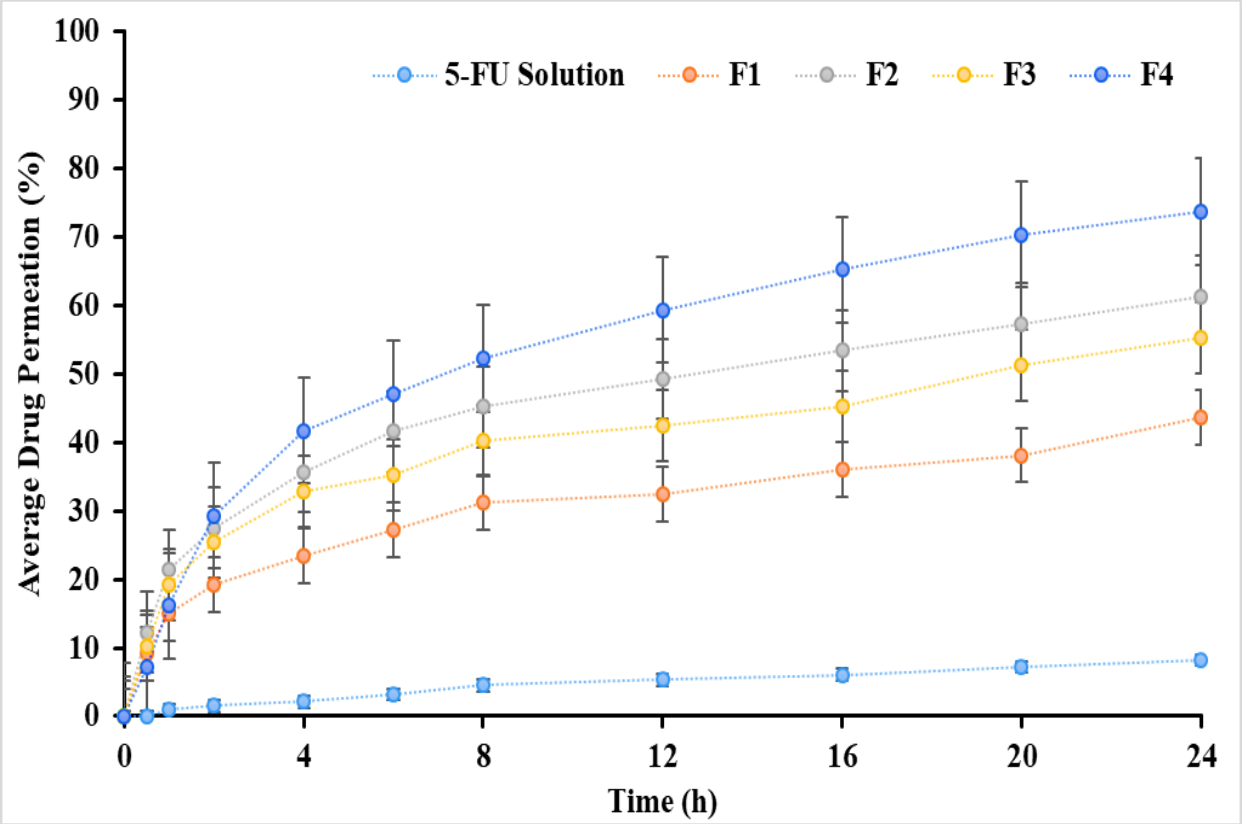

(a)
SED 20.0kV WD18mm P.C.60 HV x1,000 1µm
NCEG-UOP 0000
(b)
SED 20.0kV WD18mm P.C.60 HV x1,000 1µm
NCEG-UOP 0000
(c)
SED 20.0kV WD18mm P.C.60 HV x2,700 5µm
NCEG-UOP 0000
(d)
SED 20.0kV WD18mm P.C.60 HV x1,000 1µm
NCEG-UOP 0000

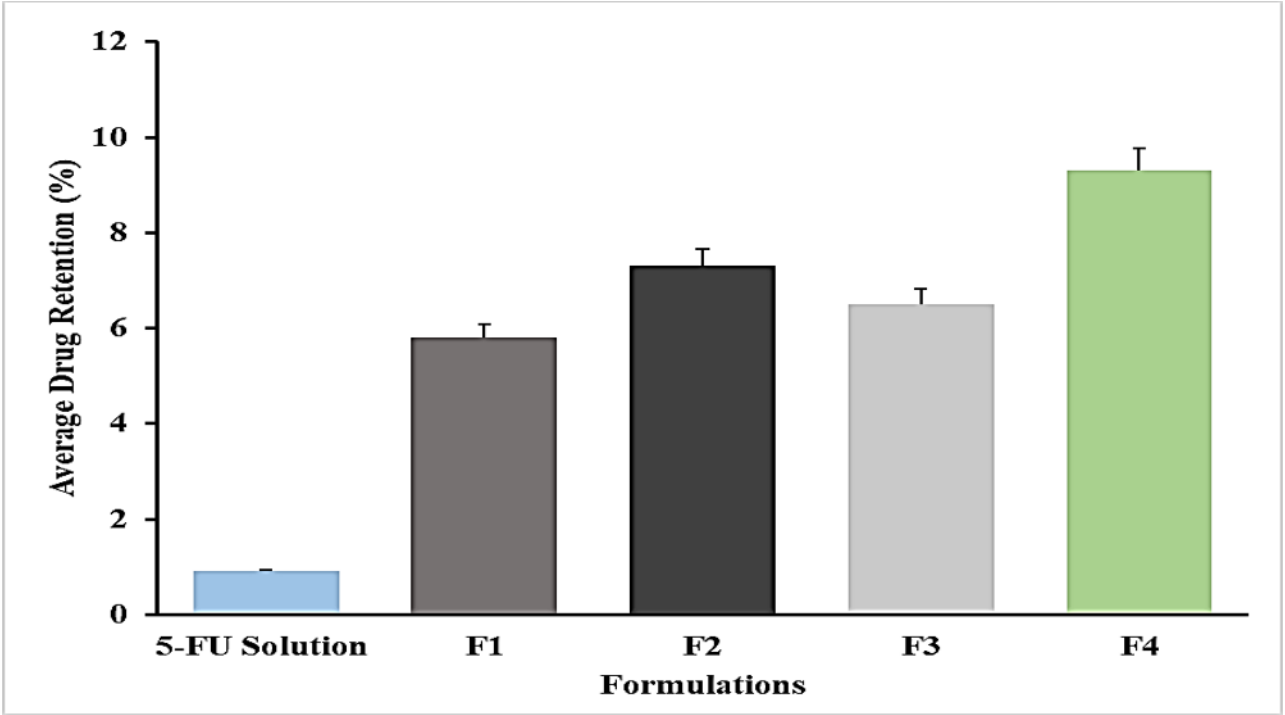

(a)
Particle Size (nm)
350
325
300
275
250
225
200
175
150
125
100
Blank-4°C
F1-4°C
F2-4°C
Blnk-25°C
F1-25°C
F2-25°C
0 day
5 days
10 days
15 days
20 days
25 days
30 days

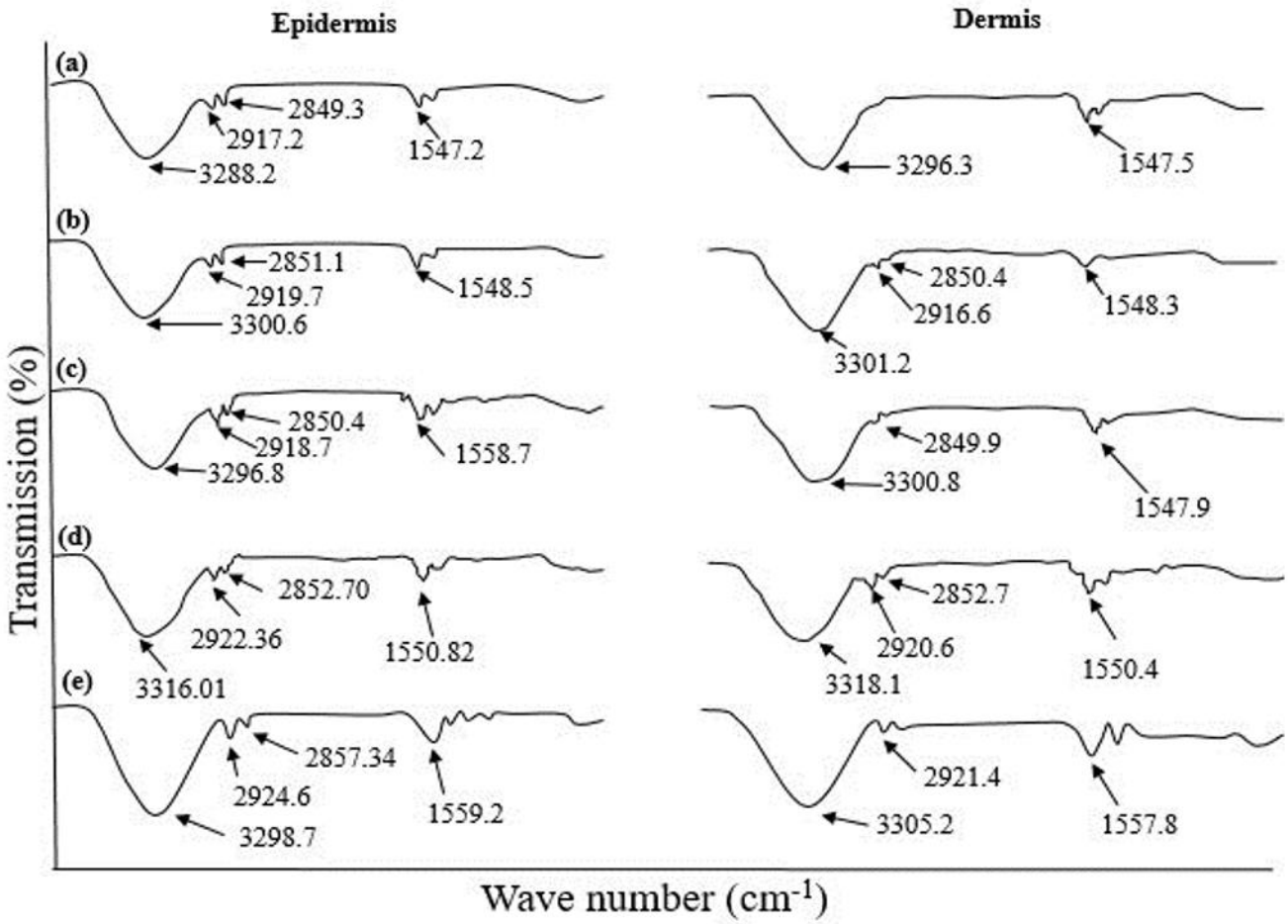

(b)
Entrapment Efficiency (%)
90
80
70
60
50
40
30
20
10
0
F1-4°C
F2-4°C
F3-4°C
F4-4°C
F1-25°C
F2-25°C
F3-25°C
F4-25°C
0 day
5 days
10 days
15 days
20 days
25 days
30 days


5
4.5
4
3.5
3
2.5
2
1.5
1
0.5
0
Erythema
Edema
F1
F2
F3
F4
Standard Irritant (Formalin)


5-FU Solution
F1
F2
F3
F4
Average Drug Release (%)
Time (h)
0
10
20
30
40
50
60
70
80
90
100
0
4
8
12
16
20
24


5-FU Solution
F1
F2
F3
F4
Average Drug Permeation (%)
Time (h)
0
10
20
30
40
50
60
70
80
90
100
0
4
8
12
16
20
24


12
10
8
6
4
2
0
Average Drug Retention (%)
5-FU Solution
F1
F2
F3
F4
Formulations


Epidermis
Dermis
(a)
2849.3
2917.2
3288.2
1547.2
3296.3
1547.5
(b)
2851.1
2919.7
3300.6
1548.5
2850.4
2916.6
3301.2
1548.3
(c)
2850.4
2918.7
3296.8
1558.7
2849.9
3300.8
1547.9
(d)
2852.70
2922.36
3316.01
1550.82
2852.7
2920.6
3318.1
1550.4
(e)
2857.34
2924.6
3298.7
1559.2
2921.4
3305.2
1557.8
Transmission (%)
Wave number (cm-1)

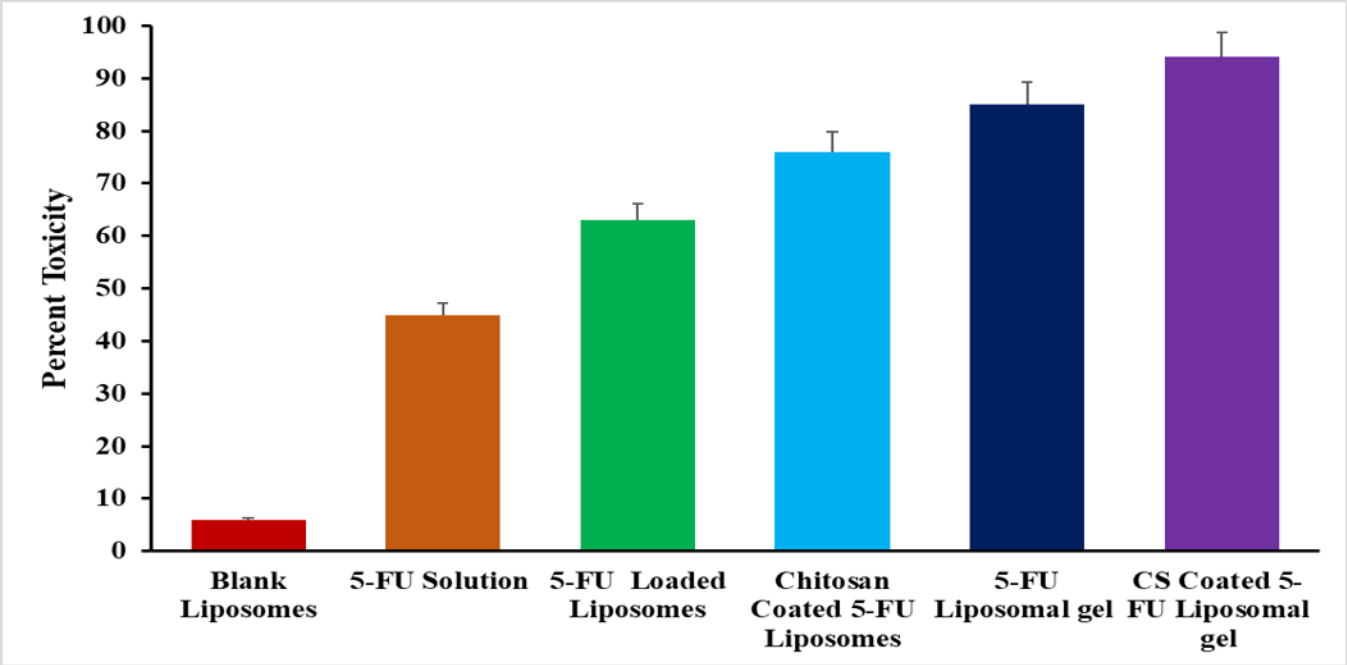


Figure 1: Particle size and zeta potential of Blank liposomes (BL), 5-FU loaded liposomes (F1) and chitosan coated 5-FU liposomes (F2).

Figure 2: ATR-FTIR analysis of (a) cholesterol, (b) Soyabean Lecithin, (c) Chitosan, d) 5-FU and (e) Liposomes respectively.

Figure 3: Scanning electron microscope images (a) 5-FU loaded liposomes (F1) (b) Chitosan-coated 5-FU liposomes (F2), 5-FU liposomal gel (F3) and (d) chitosan-coated 5-FU liposomal gel (F4).

Figure 4: Variation in particle size (F1 & F2) and entrapment efficiency of 5-FU-loaded liposomes (F1), chitosan-coated 5-FU liposomes (F2), 5-FU liposomal gel (F3), and chitosan-coated 5-FU liposomal gel (F4), storage at 4 ± 1 ℃, Mean ± SD (n = 3).

Figure 5: Irritation to the skin: the presence of erythema and edema. The data is presented as means ± standard deviations (n = 3).

Figure 6: *In vitro* release profile of 5-FU from 5-FU solution, 5-FU-loaded liposomes (F1), chitosan-coated 5-FU liposomes (F2), 5-FU liposomal gel (F3) and chitosan-coated 5-FU liposomal gel (F4) in PBS (pH 5.5) at 32 ± 0.5 ℃ (Mean ± SD (n = 3).

Figure 7: Average drug permeation (%) of the pure 5-FU solution, 5-FU loaded liposomes (F1), chitosan-coated 5-FU liposomes (F2), 5-FU liposomal gel (F3) and Chitosan-coated 5-FU liposomal gel (F4), data are expressed as mean ± S.D (n = 3).

Figure 8: 5-FU solution, 5-FU loaded liposomes (F1), chitosan-coated 5-FU liposomes (F2), 5-FU liposomal gel (F3) and chitosan-coated 5-FU liposomal gel (F4) Drug retention in skin dermis based on an *ex vivo* permeation study.

Figure 9: ATR-FTIR spectra of the epidermis and dermis (a) untreated skin epidermis and dermis (b) epidermis and dermis treated with formulation F1, (c) epidermis and dermis treated with formulation F2, (d) epidermis and dermis treated with formulation F3, (e) epidermis and dermis treated with formulation F4, data are express as mean ± S. D, n = 3.

Figure 10. Cytotoxicity profile of Blank liposomes (BL), 5-FU solution, 5-FU loaded liposomes (F1), chitosan-coated 5-FU liposomes (F2), 5-FU liposomal gel (F3) and chitosan-coated 5-FU liposomal gel formulation)F4) of different serial dilutions in B16F10 cell lines.

Supplementary Files

This is a list of supplementary files associated with this preprint. Click to download.

- GraphicalAbstract.pdf